Preparation of bulkphase nitride perovskite LaReN3 and topotactic reduction to LaNiO2type LaReN2

COMMUNICATION

Preparation of bulk-phase nitride perovskite $LaReN_3$ and topotactic reduction to $LaNiO_2$-type $LaReN_2$

Simon D. Kloß[a], Martin L. Weidemann,[b] J. Paul Attfield*[a]*

[a] Dr. S. D. Kloß, Prof. Dr. J. Paul Attfield
Centre for Science at Extreme Conditions
University of Edinburgh
Edinburgh EH9 3FD, UK
E-mail: v1skloss@ed.ac.uk
E-mail: j.p.attfield@ed.ac.uk
[b] Ludwig-Maximilians-University Munich, Department Chemistry, 81377 Munich, Germany

Supporting information for this article is given via a link at the end of the document.

Abstract: While halide and oxide perovskites are numerous and many display outstanding properties, ABN_3 perovskite nitrides are extremely rare due synthetic challenges arising from the low chemical potential of nitrogen and a tendency to form low-coordination nitridometallate anions. Here we report the preparation of a perovskite nitride $LaReN_3$ through azide-mediated oxidation at high pressure. High-resolution synchrotron diffraction shows that $LaReN_3$ has a low symmetry, triclinic, perovskite superstructure resulting from orbital ordering with strong spin-orbit coupling distortions. Topotactic reduction of $LaReN_3$ above 500 °C leads to layered tetragonal $LaReN_2$ via a probable $LaReN_{2.5}$ intermediate, the first reported examples of nitride defect-perovskites. Magnetisation and conductivity measurements indicate that $LaReN_3$ and $LaReN_2$ are both metallic solids. The two chemical approaches presented here are expected to lead to new classes of ABN_3 and defect ABN_{3-x} nitride perovskite materials.

ABX_3 perovskites based on halide or oxide anions feature important properties and applications such as in $MeNH_3PbI_3$ for photovoltaics, $BaTiO_3$ for ferroelectrics, and $La_{1-x}Sr_xMnO_3$ for colossal magnetoresistance and have been extensively investigated.[1–3] Oxide nitride perovskites, where the partial exchange of O by N narrows the bandgap, resulting in materials such as the water splitting photocatalyst $BaTaO_2N$ and red-yellow $La_{1-x}Ca_xTaO_{1+x}N_{2-x}$ pigments, are also well-studied.[4–6] These also include non-stoichiometric materials such as $LaWO_{0.6}N_{2.4}$, $SrWO_{1.63}N_{1.37}$, $EuWO_{1.58}N_{1.42}$ based on tungsten.[7] However, pure ABN_3 nitride perovskites are almost unknown, with $TaThN_3$ as the only reported bulk phase and a recent report of thin-film $LaWN_3$ as a second example although this remains to be critically distinguished from the above $LaWO_{0.6}N_{2.4}$.[8,9]

Prerequisite for stable nitride perovskites is that the cations have high formal charges, e.g. A/B = 2/7, 3/6, 4/5, to balance the anion charge while also satisfying Goldschmidt's tolerance factor ($t = r_A/\sqrt{2}(r_B + r_N) \approx 0.8$-$1.0$ where r_i are ionic radii).[10] The 3/6 combination offers many possible new materials such as rare-earth tungstates and rhenates and recent ab initio calculations have predicted properties such as ferroelectricity in $LaWN_3$ and ferromagnetism in $GdReN_3$.[11–13] The synthesis of nitrides with metals in high oxidation states is, however, challenging owed to the low energy of nitride formation, which is a fundamental problem of nitride chemistry.[14,15] The nitrogen chemical potential offered by ambient and medium pressure (<1 GPa) methods such as N_2 or NH_3 gas flow or autoclaves is low and typically metal-rich nitrides with low oxidation states are produced as demonstrated by nitride anti-perovskites and transition metal nitridometallates.[16,17]

Increasing the chemical potential of nitrogen-bearing precursors can be achieved by high pressure synthesis in the GPa range.[18,19] For example, N_2-loaded diamond-anvil-cells (DAC) were used for the preparation of noble metal nitrides, pernitrides, polynitrides and pentazolate salts, but with DACs the sample volume is very small and investigations are usually limited to binary phases.[20–22] In situ nitridation methods using large-volume-presses are far less studied, but recently bulk-phases of rocksalt-type $Mg_{0.4}Fe_{0.6}N$ and a novel highly oxidized iron(IV) nitride, Ca_4FeN_4, were reported using methods based on solid sodium azide.[23–25] Here we report that the nitride perovskite $LaReN_3$ can be prepared by this method, starting from commercial NaN_3, LaN and Re metal. We have also synthesised and characterised the layered $LaNiO_2$-type $LaReN_2$ via a post-synthetic topotactic reduction of $LaReN_3$ during which an intermediate phase that is probably $LaReN_{2.5}$ is also observed.

Reaction of LaN, Re metal, and NaN_3 (equation (1)) at 8 GPa pressure and temperatures ranging from 1000–1200 °C leads to the formation of bulk-phase $LaReN_3$. After recovering the sample from the Pt-capsule and washing with water to remove sodium, a microcrystalline air-stable powder with yield of ca. 50 mg per experiment is obtained (details in Supporting Methods).

$$LaN + Re + NaN_3 \rightarrow LaReN_3 + Na + ½\ N_2 \quad (1)$$

An elemental composition of $La_{0.95(11)}Re_{1.00(14)}N_{3.44(24)}$ was determined through EDX spectroscopy (normalized on Re, 15 datapoints averaged, Supplementary Table 1) in agreement with the nominal formula, where the apparent excess of N is likely due to the lower accuracy of EDX spectroscopy for light elements. Small amounts of detected oxygen (< 5 at-%) are attributed to surface hydrolysis owed to washing.

High-resolution powder synchrotron X-ray diffraction data (Figure 1a) show that $LaReN_3$ is almost phase pure with a small Re byproduct (ca. 1 wt-%) also observed. Fits of low symmetry and phase separated models were tried to account for broadenings and splittings of the perovskite peaks, as shown in SI, and the best fit was obtained using a single triclinic phase (space group $I\bar{1}$, a = 5.58532(6), b = 5.59484(6), c = 7.90587(8) Å, α = 89.9325(11), β = 90.1703(9), γ = 90.1536(8)°). The high scattering contrast between heavy La/Re and light N as well as peak overlap impeded free refinement of nitrogen coordinates in $I\bar{1}$ but a reliable model was obtained using atom position constraints of the monoclinic $I2/c$ space group (this simplifies the octahedral tilting from $a^-b^-c^-$ in $I\bar{1}$ to $a^-b^-b^-$ in $I2/c$ following Glazer notation).[26] Refinement results are shown in Figure 1b, with further details details in Supplementary Discussion, and Supplementary Tables 2–4.

The triclinic symmetry of $LaReN_3$ is surprising given that the Goldschmidt tolerance factor t = 0.99 based on Shannon ionic radii[27] is very close to the t = 1 value for an ideal cubic perovskite. Observation of this small triclinic distortion provides indirect evidence that $LaReN_3$ is essentially stoichiometric, as small deviations in composition are known to increase symmetry to

monoclinic as in other triclinic $I\bar{1}$ perovskites such as cation-ordered Sr_2FeIrO_6.[28]

Table 1: Re–N distances (Å) and Re1–N–Re2 angles (°) in $LaReN_3$.

	N1	N2	N3
Re1	2.021(14)	1.953(15)	1.979(1)
Re2	1.950(15)	2.024(14)	1.979(1)
Re1–N–Re2	167.7(7)	169.0(8)	174.2(13)

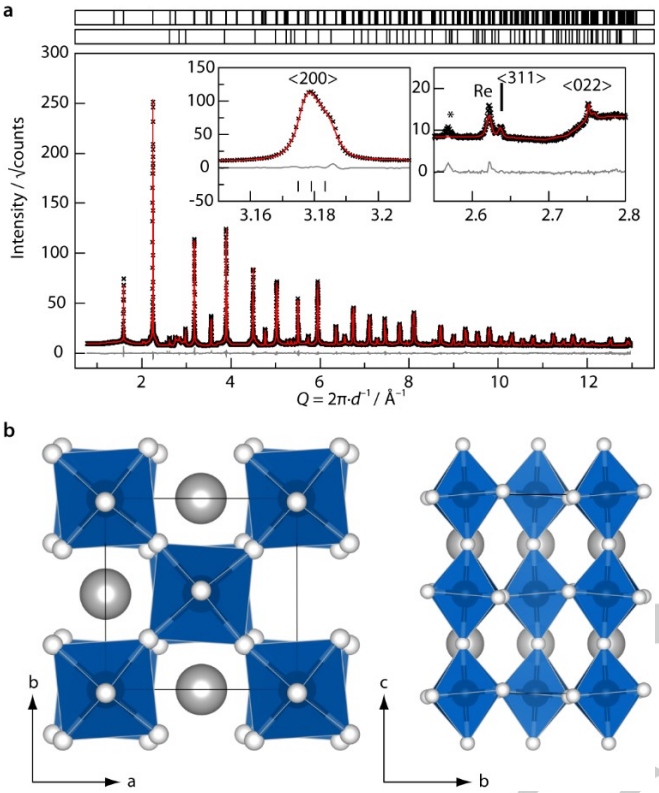

Figure 1: a Rietveld fit to 300 K synchrotron powder X-ray diffraction data of $LaReN_3$. Square root of intensity is plotted for clarity. Left inset shows triclinic splitting of the <200> reflection (indexed on a 2x2x2 supercell of the basic cubic perovskite cell). Right inset shows weak <311> and <022> superstructure intensities due to nitrogen displacements, and an impurity peak from Re (1 wt-%) and an unidentified small reflection marked with an asterisk. **b** Triclinic crystal structure of $LaReN_3$ with La/Re/N as grey/black/white spheres.

The Re–N distances (Table 1) reveal that the ReN_6 octahedra are tetragonally elongated. Jahn-Teller distortion of t_{2g}^1 systems leads to tetragonal compression but for large spin-orbit coupling, as can be expected for Re^{VI}, compression and elongation distortions become comparable in energy, as observed in A_2TaCl_6 (A = K, Rb, Cs).[29,30] It appears that the triclinic distortion of the $LaReN_3$ perovskite structure is principally a result of orbital ordering, but neutron diffraction data will be required to refine the full $I\bar{1}$ superstructure and confirm the ground state distortion.

The thermal behaviour of $LaReN_3$ was explored through X-ray powder diffraction from ambient up to 1000 °C under Ar atmosphere as well as by thermogravimetric analysis (Figure 2). As the resolution of the in-house diffractometer was insufficient to resolve the triclinic distortion, the lattice parameters of $LaReN_3$ were constrained to a cubic average and a linear expansion coefficient of α_a = 13.1(5) x 10^{-6} K^{-1} was measured up to 500 °C. This is comparable to values for oxide perovskites of similar heavy metals such as 6.93 x 10^{-6} K^{-1} for cubic $BaHfO_3$.[31]

$LaReN_3$ was found to decompose into a $LaNiO_2$-type $LaReN_2$ in the region between 500 and 620 °C (phase fractions Figure 2b) with an intermediate phase also observed.[32] Thermogravimetric analysis reveals a steady mass loss up to 600 °C with a steeper descent at 600–700°C towards the predicted weight loss for the $LaReN_3$ → $LaReN_2$ transformation. The intermediate phase is observed by X-ray diffraction at temperatures 500−540°C (with a prominent reflection at 2θ = 15° in Figure 2a) and likely corresponds to a $LaNiO_{2.5}$-type or brownmillerite-type defect perovskite $LaReN_{2.5}$. Refinement of a simple orthorhombic perovskite cell against the 520 °C X-ray pattern (Supplementary Figure 2) yielded a = 3.955(1), b = 3.946(3), c = 3.797(6) Å, which is comparable to values for $LaNiO_{2.5}$ which has a monoclinic 2a x 2b x 2c supercell with a = 3.921, b = 3.899, c = 3.736 Å and β = 93.9°.[33] However, further study by neutron diffraction will be needed to confirm the structure of $LaReN_{2.5}$.

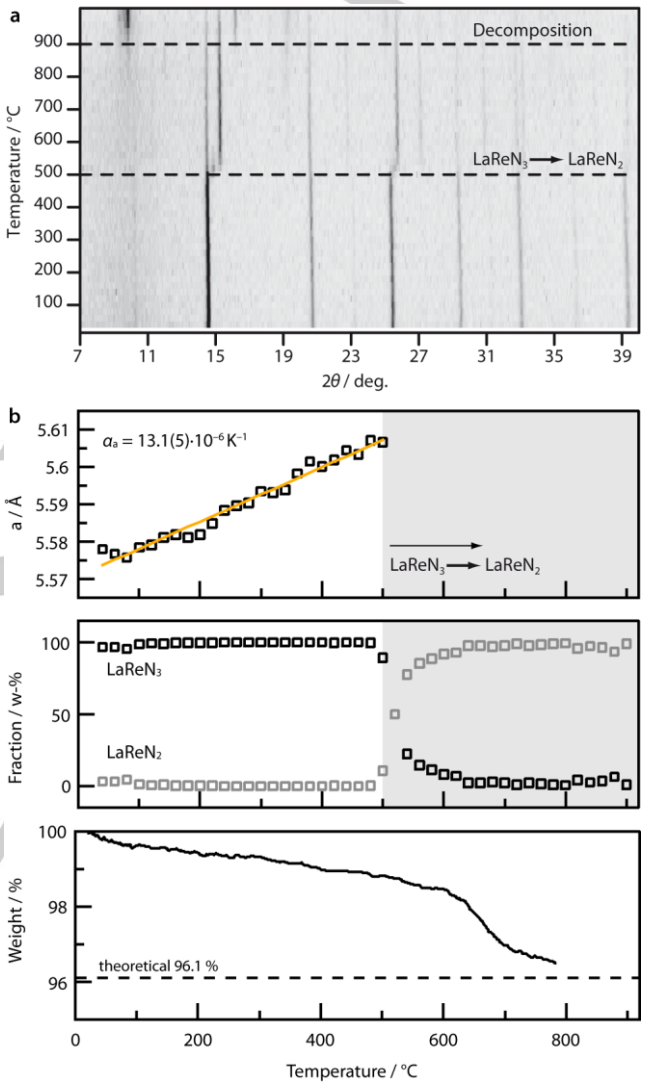

Figure 2: a Temperature-dependent powder X-ray diffraction (20 K steps, 1h measurements) with decomposition onsets indicated by horizontal dashed lines. The strong reflection appearing at 2θ = 10° above 900 °C is due to crystallization of the quartz capillary. **b** Thermal variations of; (top) averaged cubic cell parameter for $LaReN_3$ showing fitted linear thermal expansion up to 500 °C (orange line), (center) refined phase fractions of $LaReN_3$ and $LaReN_2$ ($LaReN_{2.5}$ was not included in this analysis), (bottom) mass loss from thermogravimetric analysis carried out at a heating rate of 10 K/min.

A bulk sample of polycrystalline $LaReN_2$ was prepared by heating $LaReN_3$ at 800 °C under 200 MPa N_2 pressure for 12 h. The X-ray pattern was fitted using a tetragonal $LaNiO_2$-type model (Figure 3a, space group $P4/mmm$, a = 3.9749(1), c = 3.5617(1) Å, results in Supplementary Tables 2–4). The topotactic reduction results in La-separated planes of corner sharing square planar $[Re^{III}N_{4/2}]^{3-}$ moieties (Figure 3b). Re–N distances of 1.9874(1) Å are comparable to those in $LaReN_3$ (Table 1). The square-planar coordination of Re that results from the topotactic reduction is unusual as similar complexes often adopt tetrahedral coordination, but for the lighter homologue Mn, several instances of Sr_2CuO_3-

type lanthanide- and actinide- based phases such as Ce_2MnN_3, Th_2MnN_3 and U_2MnN_3 with corner-sharing square planar $[MnN_4]$ moieties are known.[34] Some decomposition to Re metal is observed – the Rietveld refinement indicates 17 w-% Re is present but this may be overestimated as severe peak broadening makes fitting difficult.

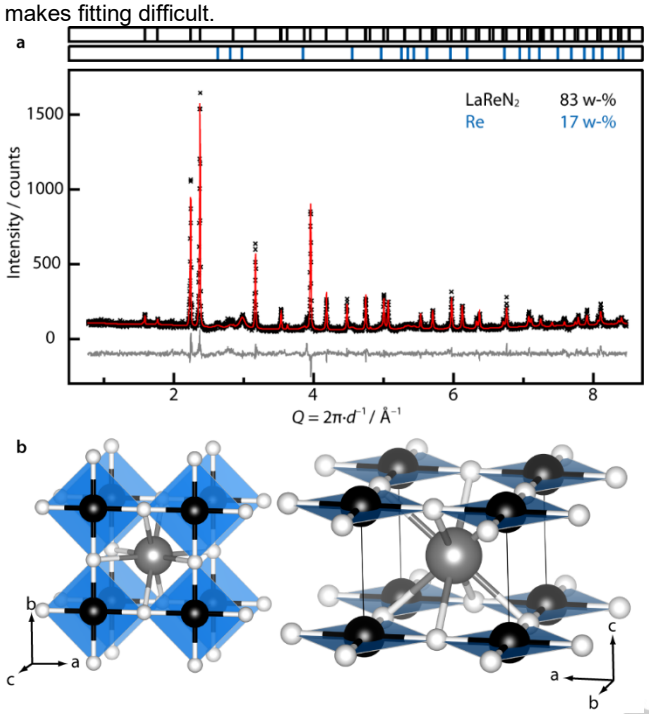

Figure 3: a Rietveld fit of the $LaReN_2$ structure to X-ray data collected on an in-house diffractometer with Mo-$K_{\alpha1}$ radiation. Re metal is also observed. **b** Views of the crystal structure of $LaReN_2$ with square planar ReN_4 units shown as blue squares.

Electronic and magnetic properties of $LaReN_3$ and $LaReN_2$ were explored through resistivity measurements on a pressed pellet of $LaReN_3$ annealed under Ar for 36 h at 400 °C, and through magnetisation measurements on the powdered samples of both phases used for X-ray structure analysis. The pellet of $LaReN_3$, which has ca. 75 % of the theoretical density, has a resistivity of ρ = 1.1 x 10^{-4} Ω·m at 300 K (Figure 4a) that remains almost constant down to 4 K, revealing intrinsic metallic behaviour with a slight increase with decreasing temperature likely due to contact or grain boundary resistances that reflect the low annealing temperature. A superconducting transition observed with T_c = 3.5 K is assigned to impurities below. The combination of metallic conductivity with strong spin-orbit coupling, as evidenced by the distorted ReN_6 octahedra within the triclinic $I\bar{1}$ superstructure, may give rise to unusual electronic properties as observed in the iridate perovskite $SrIrO_3$.[35]

$LaReN_3$ and $LaReN_2$ have temperature independent magnetic susceptibilities (Figure 4b) that are positive at high field with values 3.4 x 10^{-4} and 2.2 x 10^{-4} emu·mol^{-1} respectively at 2.2 K and 5 T, indicative of Pauli paramagnetism (Figure 4c) in keeping with metallic properties for both compounds. This is in line with DFT predictions on $LaReN_3$ and for $LaReN_2$ the truism that nitrogen-poor transition metal nitrides are usually metallic.[12] The ReN_3 framework of $LaReN_3$ is also notable as being isoelectronic with the metallic oxide ReO_3.

The superconducting transition at T_c = 3.5 K in the electric resistivity of the $LaReN_3$ sample is also seen in magnetisation measurements on the $LaReN_3$ and $LaReN_2$ samples. The transition remains visible in field-dependent resistivity measurements on $LaReN_3$ up to 5000 Oe (Figure 4a inset), in line with the field-dependent magnetisation of the $LaReN_3$ sample (Figure 4c) showing a lower critical field H_{c1} ≈ 200 Oe and upper critical field H_{c2} ≈ 6000 Oe, while the $LaReN_2$ sample shows a lower critical field of H_c ≈ 30 Oe.

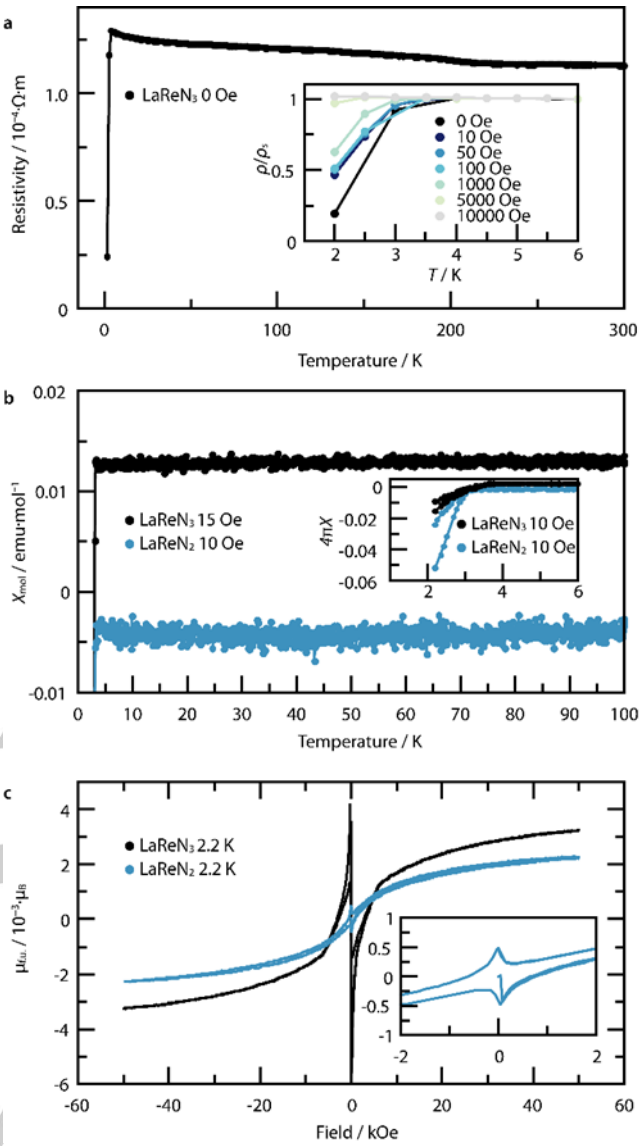

Figure 4: a Thermal variation of resistivity of a $LaReN_3$ pellet. Inset displays field-dependent measurements normalised to 6 K values ρ_s showing the impurity superconducting transition. **b** Low-temperature ZFC molar susceptibilities of powder $LaReN_3$ and $LaReN_2$ samples. The negative value for $LaReN_2$ at the low measuring field results from the small hysteresis shown in the inset to Figure 4c. Inset shows FC/ZFC (upper/lower branches) superconducting volume susceptibility fractions for a sintered sample of $LaReN_3$ (volume determined measured with digital microscope, Supplementary Figure 3) and for powdered $LaReN_2$. **c** Magnetization-field hystereses of $LaReN_3$ and $LaReN_2$ powders showing low-field features from superconducting impurities.

Magnetic shielding measurements gave a superconducting volume fraction of ~2 % for a piece of sintered $LaReN_3$ from the pellet used for electric resistivity (Supplementary Figure 3) and ~6 % for the $LaReN_2$ powder. These small fractions indicate that superconductivity probably arises from impurity phases that give rise to percolative superconduction through grain boundaries. Re metal is superconducting with properties dependent on its metallurgical history and the highest reported critical temperature and field, from high-pressure torsion experiments on Re metal discs, are T_c = 3.2 K, and H_{c2} = 1000 Oe at 2 K.[36–38] Hence the superconductivity observed in our $LaReN_2$ sample containing ~17 wt-% Re can be assigned to this secondary phase, but it does not account for the much larger H_{c2} ≈ 6000 Oe observed in our $LaReN_3$ sample. Here superconductivity may stem from ReN_x impurities as partly nitrided Re-films showed T_c's up to 5 K dependent on nitrogen-content.[39]

These results demonstrate that rhenium-based nitride perovskites can be prepared through a high-pressure azide synthesis route,

stabilising the high Re^{VI} oxidation state and overcoming the covalent multiple bonding observed in other rhenium nitrides.[40] The same approach should enable many other ABN_3 nitride perovskite based on rare-earth and possibly alkaline earth A-site cations to be prepared and likely result in the discovery of useful properties; while the superconductivity in our $LaReN_3$ and $LaReN_2$ samples was probably due to Re and ReN_x impurities, chemical tuning could induce bulk phase superconductivity and other predicted properties such as ferroelectricity in $LaWN_3$ or ferromagnetism in $GdReN_3$ can now be explored in bulk samples.[11–13]

The discovery of $LaReN_{2.5}$ and $LaReN_2$ in this work also demonstrates that post-synthetic topotactic reduction can be used to access novel ABN_{3-x} defect-perovskite nitrides via a hard-soft chemical approach.[41]. A great variety of anion-defect ordered perovskite oxides are known, often with complex long-period superstructures such as in $SrCrO_{2.8}$ prepared by a similar hard-soft chemical route,[41] and with the $YBa_2Cu_3O_7$ superconductor as a famous example amongst cation-ordered perovskites. Discovery of the layered $LaReN_2$ phase is particularly notable given observations of superconductivity in oxide analogues such as the infinite-layer cuprate $(Sr,Ca)CuO_2$ and recently-discovered $(Nd,Sr)NiO_2$.[42,43]

The high pressure and post-synthetic (hard-soft) routes used here are expected to open a new field of perovskite-based nitrides and can likely be extended to related structures such as Ruddelsden-Popper phases, leading to further new classes of functional metal nitrides.

Acknowledgements

The authors thank Dr. Stefan Rudel (LMU Munich) for the light microscope imaging, Timotheus Hohl (LMU Munich) for the TGA measurements, Prof. Dirk Johrendt (LMU Munich) for use of the PPMS, and Dr. Jonathan Wright and Dr. Catherine Dejoie for (ESRF) for synchrotron measurements. We acknowledge the DFG and EPSRC for funding.

Conflict of interest

The authors declare no competing interests.

Keywords

high-pressure chemistry, nitrides, perovskite phases, transition metals, solid-phase synthesis

References

[1] P. Wagner, G. Wackers, I. Cardinaletti, J. Manca, J. Vanacken *Phys. status solidi* **2017**, *214*, 1700394.
[2] A. S. Bhalla, R. Guo, R. Roy *Mater. Res. Innov.* **2000**, *4*, 3.
[3] Z. Fan, K. Sun, J. Wang *J. Mater. Chem. A* **2015**, *3*, 18809.
[4] M. Jansen, H. P. Letschert *Nature* **2000**, *404*, 980.
[5] A. Fuertes *APL Mater.* **2020**, *8*, 020903.
[6] H. Kageyama, K. Hayashi, K. Maeda, J. P. Attfield, Z. Hiroi, J. M. Rondinelli, K. R. Poeppelmeier *Nat. Commun.* **2018**, *9*, 772.
[7] **a** P. Bacher, P. Antoine, R. Marchand, P. L'Haridon, Y. Laurent, G. Roult, *J. Solid State Chem.* **1988**, *77*, 67. **b** M. T. Weller, S. J. Skinner, *Int. J. Inorg. Mater.* **2000**, *2*, 463. **c** R. Pastrana-Fábregas, J. Isasi-Marín, C. Cascales, R. Sáez-Puche, *J. Solid State Chem.* **2007**, *180*, 92.
[8] N. E. Brese, F. J. DiSalvo *J. Solid State Chem.* **1995**, *120*, 378.
[9] K. R. Talley, C. L. Perkins, D. R. Diercks, G. L. Brennecka, A. Zakutayev, **2020**, arXiv preprint arXiv:2001.00633.
[10] V. M. Goldschmidt *Naturwissenschaften* **1926**, *14*, 477–485.
[11] R. Sarmiento-Pérez, T. F. T Cerqueira, S, Körbel, S. Botti, M. A. L. Marques *Chem. Mater.* **2015**, *27*, 5957–5963.
[12] J. A. Flores-Livas, R. Sarmiento-Pérez, S. Botti, S., Goedecker, M. A. L. Marques *J. Phys. Mater.* **2019**, *2*, 025003.
[13] Y.-W. Fang, C. A. J. Fisher, A. Kuwabara, X.-W. Shen, T. Ogawa, H. Moriwake, R. Huang, C.-G. Duan, *Phys. Rev. B* **2017**, *95*, 014111.
[14] W. Sun, C. J. Bartel, E. Arca, S. R. Bauers, B. Matthews, B. Orvañanos, B.-R. Chen, M. F. Toney, L. T. Schelhas, W. Tumas, J. Tate, A. Zakutayev, S. Lany, A. M. Holder, G. Ceder, *Nat. Mater.* **2019**, *18*, 732.
[15] D. R. Glasson, S. A. A. Jayaweera *J. Appl. Chem.* **1968**, *18*, 65.
[16] R. Niewa *Eur. J. Inorg. Chem.* **2019**, 3647.
[17] D. H. Gregory *J. Chem. Soc. Dalt. Trans.* **1999**, *3*, 259.
[18] W. Sun, A. Holder, B. Orvañanos, E. Arca, A. Zakutayev, S. Lany, G. Ceder, *Chem. Mater.* **2017**, *29*, 6936–6946.
[19] H. Alkhaldi, P. Kroll *J. Phys. Chem. C* **2019**, *123*, 7054.
[20] E. Gregoryanz, C. Sanloup, M. Somayazulu, J. Badro, G. Fiquet, H. Mao, R. J. Hemley, *Nat. Mater.* **2004**, *3*, 294.
[21] M. Bykov, E. Bykova, G. Aprilis, K. Glazyrin, E. Koemets, I. Chuvashova, I. Kupenko, C. McCammon, M. Mezouar, V. Prakapenka, H.-P. Liermann, F. Tasnádi, A. V. Ponomareva, I. A. Abrikosov, N. Dubrovinskaia, L. Dubrovinsky, *Nat. Commun.* **2018**, *9*, 2756
[22] B. A. Steele, E. Stavrou, J. C. Crowhurst, J. M. Zaug, V. B. Prakapenka, I. I. Oleynik *Chem. Mater.* **2017**, *29*, 735.
[23] G. Serghiou, et al. *Angew. Chemie Int. Ed.* **2015**, *54*, 15109.
[24] S. D. Kloß, A. Haffner, P. Manuel, M. Goto, Y. Shimakawa, J. P. Attfield *Nat. Commun.* **2021**, *12*, 571.
[25] M. Bykov, E. Bykova, G. Aprilis, K. Glazyrin, E. Koemets, I. Chuvashova, I. Kupenko, C. McCammon, M. Mezouar, V. Prakapenka, H.-P. Liermann, F. Tasnádi, A. V. Ponomareva, I. A. Abrikosov, N. Dubrovinskaia, L. Dubrovinsky, *Nat. Commun.* **2018**, *9*, 2756.
[26] A. Glazer *Acta Crystallogr., Sect. B: Struct. Crystallogr. Cryst. Chem.* **1972**, *28*, 3384.
[27] R. D. Shannon *Acta Crystallogr., Sect. A: Cryst. Phys., Diffr., Theor. Gen. Crystallogr.* **1976**, *32*, 751.
[28] J. E. Page, C. V. Topping, A. Scrimshire, P. A. Bingham, S. J. Blundell, M. A. Hayward *Inorg. Chem.* **2018**, *57*, 10303.
[29] S. V. Streltsov, D. I. Khomskii *Phys. Rev. X* **2020**, *10*, 031043.
[30] H. Ishikawa, T. Takayama, R. K. Kremer, J. Nuss, R. Dinnebier, K. Kitagawa, K. Ishii, H. Takagi, *Phys. Rev. B* **2019**, *100*, 045142.
[31] T. Maekawa, K. Kurosaki, S. Yamanaka *J. Alloys Compd.* **2006**, *407*, 44.
[32] P. Levitz, M. Crespin, L. Gatineau *J. Chem. Soc., Faraday Trans. 2* **1983**, *79*, 1195.
[33] J. A. Alonso, M. J. Martínez-Lope, J. L. García-Muñoz, M. T. Fernández *Phys. B Condens. Matter* **1997**, *234-236*, 18.
[34] **a** R. Niewa, G. V. Vajenine, F. J. DiSalvo, H. Luob, W. B. Yelon, *Z. Naturforsch. B* **1998**, *53*, 63. **b** R. Benz, W. H. Zachariasen, *J. Nucl. Mater.* **1970**, *37*, 109.
[35] K. Sen, D. Fuchs, R. Heid, K. Kleindienst, K. Wolff, J. Schmalian, M. Le Tacon, *Nat. Commun.* **2020**, *11*, 4270.
[36] J. G. Daunt, T. S. Smith *Phys. Rev.* **1952**, *88*, 309.
[37] J. K. Hulm, B. B. Goodman *Phys. Rev.* **1957**, *106*, 659.
[38] M. Mito, H. Matsui, K. Tsuruta, T. Yamaguchi, K. Nakamura, H. Deguchi, N. Shirakawa, H. Adachi, T. Yamasaki, H. Iwaoka, Y. Ikoma, Z. Horita, *Sci. Rep.* **2016**, *6*, 36337.
[39] M. Fuchigami, K. Inumaru, S. Yamanaka *J. Alloys Compd.* **2009**, *486*, 621.
[40] A. Chaushli, C. Wickleder, H. Jacobs *Z. Anorg. Allg. Chem.* **2000**, *626*, 892.
[41] A. M. Arévalo-López, J. A. Rodgers, M. S. Senn, F. Sher, J. Farnham, W. Gibbs, J. P. Attfield, *Angew. Chem. Int. Ed.* **2012**, *51*, 10791; **2012**, *124*, 10949.
[42] M. Azuma, Z. Hiroi, M. Takano, Y. Bando, Y. Takeda *Nature*, **1999**, *356*, 775.
[43] D. Li, K. Lee, B. Y. Wang, M. Osada, S. Crossley, H. R. Lee, Y. Cui, Y. Hikita, H. Y. Hwang, *Nature* **2019**, *572*, 624.

Entry for the Table of Contents

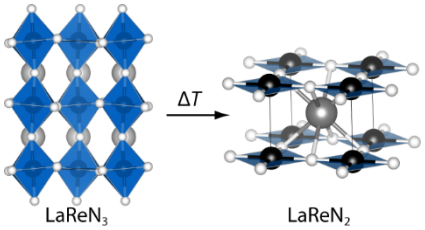

Nitride perovskites are extremely rare and challenging to synthesise, but an azide-mediated high pressure route has been used to prepare $LaReN_3$ which can be topotactically reduced to layered $LaReN_2$.